https://doi.org/10.1109/IDC.2007.374555

Sensor Fault Detection for UAVs using a Nonlinear Dynamic Model and the IMM-UKF Algorithm

Lennon Cork [1#], Rodney Walker [2]

[1] *Australian Research Center for Aerospace Automation (ARCAA), Queensland University of Technology (QUT)*
2 George Street, Brisbane, Australia, l.cork@qut.edu.au

[2] *Australian Research Center for Aerospace Automation (ARCAA), Queensland University of Technology (QUT)*
2 George Street, Brisbane, Australia, ra.walker@qut.edu.au

Abstract

This paper presents a method of Fault Detection, Identification and Accommodation for inertial sensors in Unmanned Aerial Vehicles. A nonlinear model of the aircraft's dynamics replace the traditional inertial navigation equations and is used in conjunction with the Interacting Multiple Model and the Unscented Kalman Filter for improving state estimation in presence of inertial sensor faults. Performance comparisons are made between filters using the inertial navigation equations and the dynamic model for the fault-free conditions. It is shown that a matched UKF will result in adequate state estimation regardless of the failure mode and that the IMM-UKF algorithm is a step closer to achieving the same performance. The IMM-UKF is shown capable of maintaining stable state estimates in the presence of all single inertial sensor faults.

1. Introduction

Unmanned Aerial Vehicles (UAVs) continue to lack the reliability and autonomy required for commercial viability in their proposed applications [1]. In part this is due to the UAVs inability to cope with sensor and actuator faults that occur within the flight control loop [2]. Sensor faults introduce modeling errors in the observation equations which can often cause standard filtering methods to become unstable. This paper investigates the application of the Interacting Multiple Model (IMM) and Unscented Kalman Filter (UKF) algorithms to state estimation in the presence of inertial sensor faults in UAVS; and demonstrates the performance improvement over other approaches.

Available literature on the IMM algorithm shows it to be a successful method of sensor and actuator FDIA when applied to linearized conditions of an aircraft's dynamics [3], [4]. However, when applied to the true nonlinear motion of an aircraft, the IMM algorithm can yield insufficient state estimation and fault detection performance. This is due to the prediction errors between the nonlinear and linearised equations and highlights the need for a nonlinear approach such as the IMM-UKF which is presented in this paper. An aerodynamic model enables predictions of the inertial sensor measurements to be generated, allowing for modeling of the inertial sensor faults as required by the multiple model approach. In the past, aircraft dynamic models have been used to aid navigation systems [5] and the IMM-UKF algorithm has been used for target tracking applications [6] however, the IMM-UKF is yet to appear in the literature with a nonlinear aircraft dynamic model as a method for providing fault tolerant state estimation.

The results presented in this paper were generated using a simulation environment, simulating four different filter variations for the purpose of understanding; (a) the model-mismatch errors caused by inertial sensor faults; (b) the performance improvements achieved by using an aerodynamic model instead of the traditional inertial navigation equations and; (c) the fault detection and state estimation performance of the IMM-UKF algorithm. The results show that a dynamic model can be used in place of the inertial navigation equations to improve the standard UKF performance. It is shown that a UKF matched to the faulty conditions can maintain state estimates with enough accuracy for the controller to continue tracking the desired flightpath, wheres a mismatched UKF often results in estimate and control failures.

This paper shows that the IMM-UKF algorithm can resist inertial sensor failures, resulting in better estimation accuracy and a more stable controller. In the next section, the IMM-UKF algorithm is presented in some detail. In section 3, the simulation environment, including the formulation of the aircraft dynamic equations are discussed. In section 4, the results of a number of Monte Carlo simulations are presented and finally section 5 concludes this paper.

2. IMM-UKF Algorithm

The Multiple Model approach assumes that the system obeys a discrete set of r modes of operation, where each mode is represented by a stochastic model. The true mode is unobserved and mode detection is achieved by comparing the behavior of the system to that of the different models. The behavior of the system is assessed through the observation errors resulting from a UKF matched to each mode. The observations are mode-dependent, leading to a dual (state and mode) estimation problem. In this application, each inertial sensor fault represents a different system model and the goal is to maintain an accurate state estimate in the presence of faults. Additional information for the IMM and UKF algorithms can be found in [9] and [10] respectively.

A. State and Output Equations

The mode uncertainty in the state equations is ignored since this application of the IMM-UKF algorithm specifically deals with sensor faults. The system is represented by a nonlinear and stochastic state-space model of the form;

$$\mathbf{x}(k+1) = \mathbf{f}\left[\mathbf{x}(k), \mathbf{u}(k), \mathbf{v}(k)\right] \tag{1}$$

$$\mathbf{z}(k+1) = \mathbf{g}\left[\mathbf{M}(k+1), \mathbf{x}(k+1), \mathbf{w}(k+1)\right] \tag{2}$$

Where k denotes the time step; $\mathbf{x} \in \Re^{n_\mathbf{x}}$ is the unknown state vector; $\mathbf{u} \in \Re^{n_\mathbf{u}}$ is the known control vector; and $\mathbf{z} \in \Re^{n_\mathbf{z}}$ is the known observation vector. $\mathbf{v} \in \Re^{n_\mathbf{v}}$ and $\mathbf{w} \in \Re^{n_\mathbf{w}}$ are the assumed independent, zero-mean white Gaussian state and observation noise vectors, with covariances $\mathbf{Q}(k)$ and $\mathbf{R}(k)$ respectively. Furthermore, $\mathbf{M}(k) \in \{M_i(k),\, i = 1, \ldots, r\}$ and denotes the model in effect during the sampling period ending at k. The state function $\mathbf{f} : \Re^{n_\mathbf{x}} \times \Re^{n_\mathbf{u}} \times \Re^{n_\mathbf{v}} \rightarrow \Re^{n_\mathbf{x}}$ and mode dependent output function $\mathbf{g}\left[\mathbf{M}(k+1)\right] : \Re^{n_\mathbf{x}} \times \Re^{n_\mathbf{w}} \rightarrow \Re^{n_\mathbf{z}}$ are arrays of known nonlinear equations. It is assumed that mode switching at k is a Markov process with known mode transition probabilities, given by;

$$p_{ij} = P\left\{\mathbf{M}(k+1) = \mathbf{M}_j | \mathbf{M}(k) = \mathbf{M}_i\right\} \tag{3}$$

The subscripts i and j refer to the mode in effect at the end of time steps k and $k+1$ respectively. We seek the unbiased, Minimum Mean Square Error (MMSE) estimate $\hat{\mathbf{x}}(k)$ of the state vector $\mathbf{x}(k)$. The probability that model $\mathbf{M}_i(k)$ matches the true model $\mathbf{M}(k)$ is given by the mode probability $\mu_i(k)$. The IMM-UKF algorithm runs a bank of r filters, where each filter is matched to a specific mode, resulting in a set of mode-matched state estimates $\hat{\mathbf{x}}^i(k|k)$ and estimate covariances $\mathbf{P}^i_{\tilde{\mathbf{x}}\tilde{\mathbf{x}}}(k|k)$, defined by;

$$\tilde{\mathbf{x}}^i(k|k) = \mathbf{x}^i(k) - \hat{\mathbf{x}}^i(k|k),\; i = 1, \ldots, r \tag{4}$$

$$\mathbf{P}^i_{\tilde{\mathbf{x}}\tilde{\mathbf{x}}}(k|k) = E\left[\tilde{\mathbf{x}}^i(k|k)\tilde{\mathbf{x}}^i(k|k)'\right],\; i = 1, \ldots, r \tag{5}$$

The mode-matched state estimate and estimate covariances are initialized from the steady state values of the UKF matched to the fault-free mode.

B. Mode Interaction and Mixing

The mode-matched state estimates and estimate covariances reflect the output of the filters in the previous time step. There is only one true mode and the observations of the filters that are not matched to the true mode have additional errors. The IMM attempts to minimize these errors by mixing the mode-matched estimates based on the mode probabilities $\mu(k)$ and the mode transition probabilities p_{ij}. The mixing probability $\mu_{i|j}(k|k)$ represents the probability that model $\mathbf{M}_i(k)$ is in effect at time k, given that model $\mathbf{M}_j(k+1)$ matches the true model. $\mu_{i|j}(k|k)$ is calculated by;

$$\begin{aligned} \mu_{i|j}(k|k) &= \frac{1}{c_j} p_{ij}\mu_i(k),\; i, j = 1, \ldots, r \\ c_j &= \sum_{i=1}^{r} p_{ij}\mu_i(k),\; j = 1, \ldots, r \end{aligned} \tag{6}$$

The mixed initial condition (state estimate $\hat{\mathbf{x}}^{0j}(k|k)$ and $\mathbf{P}^{0j}_{\tilde{\mathbf{x}}\tilde{\mathbf{x}}}(k|k)$ covariance) for the filter matched to model $\mathbf{M}_j(k+1)$ is then calculated by;

$$\hat{\mathbf{x}}^{0j}(k|k) = \sum_{i=1}^{r} \hat{\mathbf{x}}^i(k|k)\mu_{i|j}(k|k),\; j = 1, \ldots, r \tag{7}$$

$$\begin{aligned} \mathbf{P}^{0j}_{\tilde{\mathbf{x}}\tilde{\mathbf{x}}}(k|k) = \sum_{i=1}^{r} \mu_{i|j}(k|k)\Big\{\mathbf{P}^i_{\tilde{\mathbf{x}}\tilde{\mathbf{x}}} + \left[\mathbf{x}^i(k|k) - \mathbf{x}^{0j}(k|k)\right] \\ \left[\mathbf{x}^i(k|k) - \mathbf{x}^{0j}(k|k)\right]'\Big\},\; j = 1, \ldots, r \end{aligned} \tag{8}$$

These initial conditions are used as inputs to the filter matched to model $\mathbf{M}_j(k+1)$ using $\mathbf{z}(k+1)$ to yield $\hat{\mathbf{x}}^j(k+1|k+1)$ and $\mathbf{P}^j_{\tilde{\mathbf{x}}\tilde{\mathbf{x}}}(k+1|k+1)$. This is achieved using a filtering algorithm which in this case is the UKF.

C. Mode-Matched Filtering

The UKF is a nonlinear extension of the Kalman Filter and is based on the principle that it is easier to approximate a probability distribution than an arbitrary nonlinear function [7]. The UKF propagates a set of weighted sigma points through the state and output equations. The sigma points are then used to estimate the means and covariances of the states and observations, which are in turn used to filter the predicted states.

In this section the mode index i or j used for the IMM algorithm are removed and an augmented state estimate and state covariance matrix is constructed;

$$\mathbf{x_a}(k) = \left[\begin{array}{ccc} \hat{\mathbf{x}}(k)' & \bar{\mathbf{v}}(k)' & \bar{\mathbf{w}}(k+1)' \end{array}\right]' \tag{9}$$

$$\mathbf{P}_{\tilde{\mathbf{a}}\tilde{\mathbf{a}}}(k) = \left[\begin{array}{ccc} \mathbf{P}_{\tilde{\mathbf{x}}\tilde{\mathbf{x}}}(k|k) & 0 & 0 \\ 0 & \mathbf{Q}(k) & 0 \\ 0 & 0 & \mathbf{R}(k+1) \end{array}\right] \tag{10}$$

The sigma points $\mathbf{X_a}(k)$ and their weightings $\mathbf{G_a}(k)$ are calculated using the unscented transform (UT) [7] given by;

$$\mathbf{X_a}(k) = \left\{ \begin{array}{l} \mathbf{x_a}(k),\; i = 0 \\ \mathbf{x_a}(k) \pm \left(\sqrt{(n_\mathbf{a} + \kappa)\,\mathbf{P}_{\tilde{\mathbf{x}}\tilde{\mathbf{x}}}(k)}\right)_i,\; i = 1, \ldots, 2n_\mathbf{a} \end{array}\right. \tag{11}$$

$$\mathbf{G_a}(k) = \left\{ \begin{array}{l} \kappa / \left(n_\mathbf{a} + \kappa\right),\; i = 0 \\ 1 / \left(2\left(n_\mathbf{a} + \kappa\right)\right),\; i = 1, \ldots, 2n_\mathbf{a} \end{array}\right. \tag{12}$$

Where i now refers to the sigma point index and corresponds the the row or column values of the matrix that is indexed. The length of the augmented state estimate is $n_\mathbf{a} = (n_\mathbf{x} + n_\mathbf{v} + n_\mathbf{w})$ and κ is the unscented transform scaling factor [7]. The sigma points can be broken into the respective state and noise components by;

$$\mathbf{X_a}(k) = \left[\begin{array}{ccc} \mathbf{X}(k)' & \mathbf{V}(k)' & \mathbf{W}(k+1)' \end{array}\right]' \tag{13}$$

The $2n_\mathbf{a} + 1$ sigma points are then propagated through the state and output equations from (1) and (2);

$$\mathbf{X}_i(k+1|k) = \mathbf{f}\left[\mathbf{X}_i(k), \mathbf{u}(k), \mathbf{V}_i(k)\right],\; i = 1, \ldots, 2n_\mathbf{a} \tag{14}$$

$$\mathbf{Z}_i(k+1|k) = \mathbf{g}\left[\mathbf{X}_i(k+1), \mathbf{W}_i(k+1)\right],\; i = 1, \ldots, 2n_\mathbf{a} \tag{15}$$

The state and output means are calculated by;

$$\hat{\mathbf{x}}(k+1|k) = \sum_{i=0}^{2n_{\mathbf{a}}} \mathbf{X}_i(k+1|k)\mathbf{G}_{\mathbf{a}_i}(k) \tag{16}$$

$$\hat{\mathbf{z}}(k+1|k) = \sum_{i=0}^{2n_{\mathbf{a}}} \mathbf{Z}_i(k+1|k)\mathbf{G}_{\mathbf{a}_i}(k) \tag{17}$$

The state and output covariances are calculated by;

$$\begin{aligned}\mathbf{P}_{\tilde{x}\tilde{x}}(k+1|k) = \sum_{i=0}^{2n_{\mathbf{a}}} \Big\{ &[\mathbf{X}_i(k+1|k) - \hat{\mathbf{x}}(k+1|k)] \\ &[\mathbf{X}_i(k+1|k) - \hat{\mathbf{x}}(k+1|k)]' \Big\} \mathbf{G}_{\mathbf{a}_i}(k)\end{aligned} \tag{18}$$

$$\begin{aligned}\mathbf{P}_{\tilde{x}\tilde{z}}(k+1|k) = \sum_{i=0}^{2n_{\mathbf{a}}} \Big\{ &[\mathbf{X}_i(k+1|k) - \hat{\mathbf{x}}(k+1|k)] \\ &[\mathbf{Z}_i(k+1|k) - \hat{\mathbf{z}}(k+1|k)]' \Big\} \mathbf{G}_{\mathbf{a}_i}(k)\end{aligned} \tag{19}$$

$$\begin{aligned}\mathbf{P}_{\tilde{z}\tilde{z}}(k+1|k) = \sum_{i=0}^{2n_{\mathbf{a}}} \Big\{ &[\mathbf{Z}_i(k+1|k) - \hat{\mathbf{z}}(k+1|k)] \\ &[\mathbf{Z}_i(k+1|k) - \hat{\mathbf{z}}(k+1|k)]' \Big\} \mathbf{G}_{\mathbf{a}_i}(k)\end{aligned} \tag{20}$$

Where $\mathbf{P}_{\tilde{z}\tilde{z}}(k+1|k)$ and $\mathbf{P}_{\tilde{x}\tilde{z}}(k+1|k)$ are the innovation and the state-observation covariances. The filter innovation (observation error) is defined by;

$$\tilde{\mathbf{z}}(k+1) = \mathbf{z}(k+1) - \hat{\mathbf{z}}(k+1|k) \tag{21}$$

The updated/filtered state estimate and covariance is then;

$$\hat{\mathbf{x}}(k+1|k+1) = \hat{\mathbf{x}}(k+1|k) + \mathbf{K}(k+1)\tilde{\mathbf{z}}(k+1) \tag{22}$$

$$\begin{aligned}\mathbf{P}_{\tilde{\mathbf{x}}\tilde{\mathbf{x}}}(k+1|k+1) = \mathbf{P}_{\tilde{\mathbf{x}}\tilde{\mathbf{x}}}(k+1|k) + \Big[&\mathbf{K}(k+1) \\ &\mathbf{P}_{\tilde{\mathbf{z}}\tilde{\mathbf{z}}}(k+1|k)\mathbf{K}(k+1)'\Big]\end{aligned} \tag{23}$$

Where, $\mathbf{K}$ is the Kalman filter gain, calculated by;

$$\mathbf{K}(k+1) = \mathbf{P}_{\tilde{\mathbf{x}}\tilde{\mathbf{z}}}(k+1|k)\mathbf{P}_{\tilde{\mathbf{z}}\tilde{\mathbf{z}}}(k+1|k)^{-1} \tag{24}$$

Finally the likelihood function of the filter (based on the innovation), under Gaussian assumptions is given by;

$$\Lambda(k+1) = |2\pi\mathbf{P}_{\tilde{\mathbf{z}}\tilde{\mathbf{z}}}|^{-1/2}\, e^{1/2(\tilde{\mathbf{z}}'\mathbf{P}_{\tilde{\mathbf{z}}\tilde{\mathbf{z}}}^{-1}\tilde{\mathbf{z}})} \tag{25}$$

Equations (9) to (25) are calculated for each model $\mathbf{M}_j$ starting with the mixed initial conditions for that model. This results in r model matched state estimates and covariances with r likelihoods (i.e. the UKF is run r times, once for each mode).

D. Mode Estimate Combination

Because model-mismatch introduces errors in the observations, the likelihood of the observation is reduced in the mismatched filters and giving a relative measure of the error in the observations between models. The resulting model probability is given by;

$$\begin{aligned}\mu_j(k+1) =& \frac{1}{c}\Lambda_j(k+1)c_j,\ j = 1,..,r \\ c =& \sum_{j=1}^{r} \Lambda_j(k+1)c_j\end{aligned} \tag{26}$$

The state estimates and covariances are updated using the model probabilities to align the estimates with the observation errors;

$$\mathbf{x}(k+1|k+1) = \sum_{j=1}^{r} \hat{\mathbf{x}}^j(k+1|k+1)\mu_j(k+1) \tag{27}$$

$$\begin{aligned}\mathbf{P}_{\tilde{\mathbf{x}}\tilde{\mathbf{x}}}(k+1|k+1) = \sum_{j=1}^{r} \mu_j(k+1)\Big\{&\mathbf{P}^j_{\tilde{\mathbf{x}}\tilde{\mathbf{x}}}(k+1|k+1) \\ &+ \big[\hat{\mathbf{x}}^i(k+1|k+1) - \hat{\mathbf{x}}^{0j}(k+1|k+1)\big] \\ &\big[\hat{\mathbf{x}}^i(k+1|k+1) - \hat{\mathbf{x}}^{0j}(k+1|k+1)\big]'\Big\}\end{aligned} \tag{28}$$

A block diagram of the IMM-UKF algorithm is shown in Fig. 1. The IMM algorithm is decision free and the algorithms undergo soft-switching[1] according to the latest updated mode probabilities.

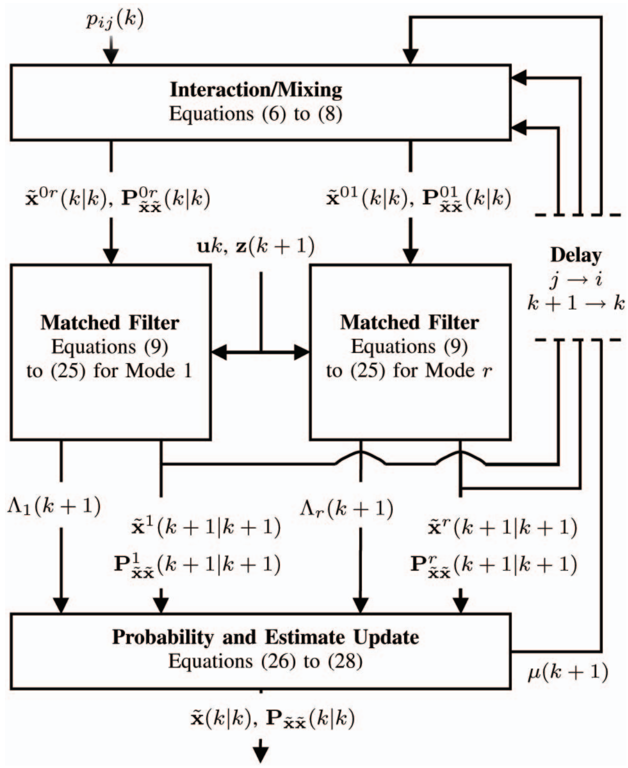

Fig. 1: IMM-UKF Algorithm

3. Simulation Environment

Testing of fault tolerant algorithms in a practical environment is a difficult task since it requires a system where the faults have minimal consequence on the operation of the system but where they can also be readily observed. This is obviously not the case for UAVs as faults within the flight control loop can have serious consequences. A simulation environment was therefore used to investigate the effects of faults on the IMM-UKF algorithm.

[1]The algorithm undergoes mixing dependent on probability instead of hard switching between the estimates of the different filters

The equations used to model the UAV's behavior were based on standard formulations of aircraft dynamics, similar to those presented in [5]. The formulation of these dynamic equations can be found in detail in texts on aircraft systems [8]. Due to the inherently complex nature of the equations governing aircraft motion, assumptions are made to reduce their complexity. Errors are introduced whenever assumptions are made, so to understand the dynamic model used in this investigation, the assumptions worth noting are;

- The equations of motion were formulated for a rigid-body and a oblate (WGS-84), non-rotating earth;
- The mass and moments of inertia of the aircraft were assumed known and constant;
- A linear relationship was assumed between throttle and the propulsive moments and forces;
- Aerodynamic forces and moments were calculated from known aerodynamic coefficients;
- Wind effects such as gust and turbulence were not considered;

The state equations represent the differential relationships of the states in continuous time. The states were integrated numerically, resulting in a discrete simulation which was run at 100Hz. The primary source of uncertainty in the aircraft dynamic model is due to errors in the calculation of the forces and moments acting on the aircraft. In the inertial navigation equations the primary source of uncertainty results from noise on the inertial sensors. For this investigation the uncertainty in the aircraft dynamic model was assumed two orders of magnitude greater than that experienced by the inertial sensors. The reason for this was to give a level of uncertainty in the state equations that represents the assumptions made.

The modeled sensor suite consisted of six inertial sensors outputting accelerations and angular rates and a GPS receiver outputting position and velocity. Inertial sensor failures were modeled by zeroing the measurement associated with the faulty sensor. Sensor noise was still included on the zeroed measurement to add uncertainty to the fault models. A filter matched to a specific sensor model excludes the fault sensor measurement so it has no feedback in the state update of the filter. The inertial sensors provided data at 100Hz and the GPS receiver provided data at 1Hz. Uncertainty was added to the outputs after sampling and was based on a typical sensor suite of a UAV [11]. In order to fully understand the performance of the proposed IMM-UKF algorithm, four filters variations were simulated;

- UKF-1 used an aerodynamic model and is matched to the true mode of the system. Simulated against all combinations of inertial sensor failures.
- UKF-2 used an aerodynamic model and is matched to the fault-free mode of the system (resulting in model mismatch when faults occur). Simulated against all combinations of inertial sensor failures.
- UKF-3 used an inertial model (traditional INS equations), matched to the fault-free mode of the system (resulting in model mismatch when faults occur). Simulated against all combinations of inertial sensor failures
- UKF-4 used an aerodynamic model, running the IMM-UKF algorithm comprising of bank of 7 filters matched to the failure modes of the accelerometers, rate gyros and the fault free mode. Simulated against all single failure modes of the inertial sensors (not including multiple failure scenarios).

The UKF-IMM algorithm was not tested for multiple sensor failures as it requires either an extremely large model set to be run in the IMM algorithm or a model selection algorithm. A number of selection algorithms can be found in the literature, however the focus of this paper was the ability of the IMM-UKF to detect and cope with single inertial failures.

4. Results

The purpose of this investigation was to explore the application of the IMM-UKF algorithm to sensor FDIA within the flight control loop of a UAV. The challenge is maintaining accurate state estimates in the presence of sensor faults. When the estimated states diverge from their true values, the errors are propagated through the flight control loop which can cause the system to behave unpredictably. The level to which a fault affects the UAVs flight performance is dependent on the resulting state errors and how those errors are propagated to the final controller output.

A. Modeling Method

The approach presented in this paper uses an aerodynamic model to predict the UAVs states. When the system is operating under fault free conditions both the UKF-2 and UKF-3 are matched to the true mode of the system and any difference in their estimation or control performance is a result from the use of the aircraft dynamic model instead of the inertial navigation equations. Table 1 gives the typical position and attitude, estimate and controll errors of UKF-2 and UKF-3 when there are no inertial sensor failures.

TABLE 1: TYPICAL ERRORS FOR THE UKF-2 AND UKF-3

Result		Position Error (m)		Attitude Error (deg)	
		UKF-2	UKF-3	UKF-2	UKF-3
Est. Error	Max	3.0833	2.5296	0.4788	1.010
	MSE	43.8296	43.2306	2.5553	13.6482
Ctr. Error	Max	0.2058	3.5180	2.8067	23.99
	MSE	19.3762	52.0945	21.9621	369.8632

In Table 1 "Max" refers to the maximum error experienced at an point in time and MSE refers to the Mean Squared Error over the duration of the simulation. The position error is calculated from the latitude, longitude and altitude statistics and the attitude error is calculated from the roll, pitch and yaw statistics. The results show that UKF-2 performs slightly better than UKF-3 as it results in a smaller MSE in both estimation and control. This is to be expected as the aircraft dynamic model provides additional information about the rates and accelerations of the aircraft. However, this is only true when the system is operating under fault free conditions.

B. Model Mismatch

When investigating the possible failure scenarios of the six inertial sensors, there are a total of 64 combinations of different faults. The results shown in Table 2 summarize how modeling errors caused by the inertial sensor faults affect the performance of the UAV when using the different filter variations

TABLE 2: UKF STABILITY IN VARYING FAULT CONDITIONS

Fault Condition			Filter			
N	I	C	UKF-1	UKF-2	UKF-3	UKF-4
0x	1	None	√	√	√	√
	All filters are stable when there are no faults					
1x	2-4	-	√	√	√	√
	5	4	√	×	×	√
	6	5	√	√	√	√
	7	6	√	×	×	√
	UKF-1/4 stable for all. UKF-2/3 unstable for 2/6					
2x	8-9	-	√	×	×	n/a
	10	1,4	√	√	√	n/a
	11	1,5	√	×	×	n/a
	12	1,6	√	√	√	n/a
	13-17	-	√	×	×	n/a
	18	3,5	√	√	√	n/a
	19-22	-	√	×	×	n/a
	UKF-1 stable for all. UKF-2/3 unstable for 12/15					
3x	23	1-3	√	×	×	n/a
	24	1-2,4	√	√	√	n/a
	25	1-2,5	√	×	×	n/a
	26-27	-	√	√	√	n/a
	28	1,3,5	√	×	×	n/a
	29-33	-	√	×	×	n/a
	34	2-3,5	√	√	√	n/a
	35-42	-	√	×	×	n/a
	UKF-1 stable for all. UKF-2/3 unstable for 17/20					
4-6x	43-64	-	√	×	×	n/a
	UKF-1 stable for all. UKF-2/3 unstable for 22/22					

In Table 2 the heading "N" refers to the number of simultaneous faults, "I" refers to the fault index and "C" refers to the fault combination of the 6 (x,y,z,p,q,r) inertial sensors. A "√" indicates the ability of the UAV to maintain flight under the specified fault condition and a "×" indicates a critical failure. For example, a dual failure of the x accelerometer and the q rate gyro (N = 2, I = 11, C = 1,5) results in failure of the system using UKF-2 and UKF-3.

It would be expected that UKF-2 and UKF-3 fail for every inertial sensor fault. This is not the case due to the fact that in some fault scenarios, the behavior of the UAV can still be captured within the uncertainty of the observations. Different sensor faults such as drift, bias or ramp faults would most likely cause filter instability, as would high dynamic maneuvers. The results obtained from simulation of the various faults for are summarized by the following points;

- UKF-1 preforms best in all fault combinations and was still able to track the true state regardless of any single or multiple inertial sensor fault. UKF-4 performed nearly as well as UKF-1 and was able to track the true state regardless of any single inertial sensor fault.
- UKF-1 and UKF-4 have greater estimation and control error under faulty conditions due to the loss of information from the failed sensors.
- All filters perform worse under rate gyro failures due there being no correcting sensors for the attitude states. This is also due to feedback of the increased attitude errors within the flight control loop.
- When operating under the fault free conditions, UKF-2 performs slightly better than UKF-3 due to the additional information provided by the aerodynamic model. The performance improvement is limited by the uncertainty in the force and moment predictions for the aircraft.
- When operating in faulty conditions, UKF-2 and UKF-3 will both become unstable unless the dynamics can be captured by the uncertainty in the state equations.

It is important to note that performance of the UAV using UKF-2 and UKF-3 is not guaranteed for any of the given fault scenarios. Due to the fact that UKF-1 performed well under all failures, the potential for providing an accurate state estimate under all of the simulated fault conditions exists however, this requires knowledge of the true mode of the system.

C. IMM-UKF Performance

The IMM-UKF algorithm attempts to estimate the true mode of the system and provide accurate state estimates based on the mode probabilities. The mode probabilities can then be tested to give an estimate of the true mode of the system. Investigation of the IMM-UKF was limited to single failures only, giving a total of seven modes that were simulated. The results shown in Table 3 give the estimation and control performance of the IMM-UKF algorithm as compared to the UKF-1 for single failure modes of the inertial sensors. The results are presented in a similar manner as in Table 1.

TABLE 3: TYPICAL ERRORS FOR THE UKF-1 AND IMM-UKF (UKF-4)

Fault	Result		Position Error (m)		Attitude Error (deg)	
			UKF-1	UKF-4	UKF-1	UKF-4
None	Est.	Max	3.0833	1.6346	0.4788	0.4516
	Error	MSE	43.8296	24.9701	2.5802	1.4096
	Ctr	Max	0.2058 .	0.1332	8.8151	0.7908
	Error	MSE	19.3762	7.0894	31.3765	4.8834
x	Est.	Max	3.3089	1.3433	0.4655	0.5169
	Error	MSE	45.4478	26.802	2.7127	1.6441
	Ctr.	Max	0.241	0.3086	9.2025	6.4197
	Error	MSE	21.7151	16.2226	39.2664	18.3564
y	Est.	Max	3.5244	2.3458	0.4467	0.9275
	Error	MSE	42.8911	33.2663	2.5943	4.8439
	Ctr.	Max	0.2362	0.2326	4.5117	4.5282
	Error	MSE	19.7247	12.9333	16.1419	19.0328
z	Est.	Max	1.505	3.0211	0.47	1.4849
	Error	MSE	42.6041	27.0744	2.6119	7.5012
	Ctr.	Max	0.1758	0.5274	2.6774	16.7799
	Error	MSE	14.801	19.2425	18.2685	86.6483
p	Est.	Max	7.6712	1.2803	0.5794	0.4855
	Error	MSE	42.5428	25.4049	7.7757	4.3161
	Ctr.	Max	0.1891	0.4688	6.2736	3.6953
	Error	MSE	17.5409	15.894	34.3969	17.73
q	Est.	Max	2.972	1.7612	0.5787	0.717
	Error	MSE	43.8074	26.3737	4.3261	6.0947
	Ctr.	Max	0.2695	0.452	8.0441	8.5438
	Error	MSE	17.2756	15.7394	33.6483	47.8768
r	Est.	Max	3.5209	4.9861	0.4931	0.5423
	Error	MSE	46.7518	72.3318	2.676	5.0983
	Ctr.	Max	0.2944	1.5287	3.6936	13.246
	Error	MSE	18.2789	55.2584	18.9034	58.0876

The results presented in Table 3 show that the IMM-UKF algorithm can be used as a fault tolerant approach to state estimation in UAVs as the system maintains adequate estimation and control performance in all single inertal sensor failures. However, the results do not indicate the accuracy of the mode estimation. The simulations of the IMM-UKF algorithm performed in this investigation dealt with single inertial sensor faults and as such model switching was not required to asses the approaches performance. The model estimation performance of the IMM-UKF algorithm is linked to the mode transition probabilities and other IMM parameters. Figure 2 shows the model probabilities as generated by the IMM-UKF algorithm when simulating a q rate gyro failure. The figure shows that with an appropriate threshold, fault detection can be achieved.

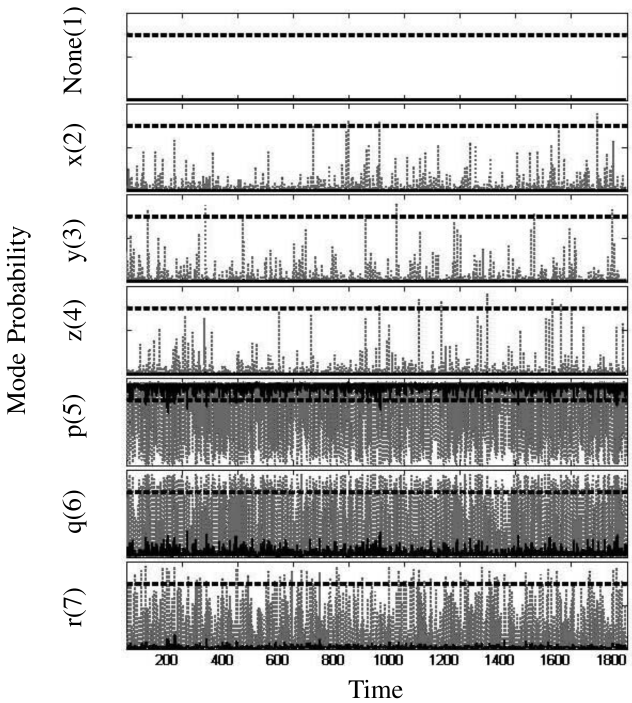

Fig. 2: Model Probabilities for failure mode 5

5. Conclusion

This paper presented results from an investigation of the IMM-UKF algorithm and its application to estimation in UAVs. The investigation focused on inertial sensor faults and their effect on the control and estimation performance of the UAV system. Four filter variations were considered demonstrating that errors resulting form inertial sensor faults can cause failures within the flight control loop and that the IMM-UKF can be used to avoid this problem. Future works includes improving the robustness of the IMM-UKF algorithm by focusing on reducing the mode probability ambiguities and implementing a model selection algorithm to reduce mode-mismatch errors, allowing the algorithm to be applied to multiple failure scenarios.

References

[1] "UAV Roadmap 2005", Office of the Secretary of Defense, Aug. 2005, pp. 213,

[2] "Unmanned Aerial Vehicle Reliability Study", Office of the Secretary of Defense, Feb. 2003, pp. 84,

[3] C. Rago, R. Prasanth, R.K. Mehra, and R. Fortenbaugh, "Failure detection and identification and fault tolerant control using the IMM-KF with applications to the Eagle-Eye UAV", presented at Decision and Control, 1998. Proceedings of the 37th IEEE Conference on, 1998.

[4] Y. Zhang and X. Rong Li, "Detection and diagnosis of sensor and actuator failures using interacting multiple model estimator", presented at Decision and Control, 1997. Proceedings of the 37th IEEE Conference on, 1997.

[5] M. Koifman and I. Y. Bar-Itzhack, "Inertial navigation system aided by aircraft dynamics", *Control Systems Technology, IEEE Transactions on*, vol. 7, pp. 487-493, 1999.

[6] N. Chi, L. Hong and J.R. Layne, "A comparison of nonlinear filtering approaches with and application to ground tracking", *Signal Processing*, vol. 85, 2005.

[7] S. J. Julier and J. K. Uhlmann, "A general method for approximating nonlinear transformations of probability distributions" Dept. of Engineering Science, University of Oxford 1996.

[8] B. L. Stevens and F. L. Lewis, *Aircraft Control and Simulation*, 2nd ed. Hoboken, New Jersey: Wiley, 2003.

[9] Y. Bar-Shalom, X. Rong Li and T. Kirubarajan, *Estimation with Applications to Tracking and Navigation*, New York: Wiley, 2001.

[10] R. Merwe, A. Doucety, N. Freitasz and E. Wan "The Unscented Particle Filter", In Advances in Neural Information Processing Systems (NIPS13), December 2000

[11] (2006) the Crossbow Technology website [online], Available: http://www.xbow.com/